

produced in half of the pollinations scored (9/19), and most other pollinations (6/19) produced three pollen tubes. Of 23 crosses allowed to mature, nine resulted in the development of three or four seeds, and 68% of these seeds germinated. Pollination with *qrt2* tetrads resulted in similar seed yields. These results with *Arabidopsis* are promising because, in some plant species, pollination with one or a few pollen grains rarely produces seeds (13). Thus, tetrad analysis in *Arabidopsis* can make use of phenotypes both of the pollen and the progeny. Moreover, tetrad analysis in plants does not require the microdissection typical of many microbial systems.

What is the nature of the biochemical defect that leads to tetrad formation? Most plants produce pollen monads, but a few species (such as water lilies, cattails, heath, and evening primrose) which are not widely used for genetic analysis release pollen in a tetrad form (14). The potential usefulness of these pollen tetrads was recognized early, but efforts to carry out tetrad analysis were hindered by technical difficulties (13). The capacity to form pollen tetrads has arisen many times through evolution and is viewed as an example of evolutionary convergence (14). In plants that form pollen monads, pollen mother cells secrete callose (a β -1 \rightarrow 3 glucan) as the daughter cells undergo cytokinesis, so that a callose wall separates each meiotic product (Fig. 1K) (15). After the developing pollen grains have initiated synthesis of the exine, the callose wall disappears (16). In those species that produce permanent pollen tetrads, the callose wall often is absent or prematurely dissolves (14).

No obvious defect in callose wall synthesis was observed in pollen from *qrt1* strains (Fig. 1L). In contrast, *qrt2* plants deposited only patches of callose between the developing microspores (Fig. 1M), potentially leading to exine fusion. Further characterization of the mechanism that gives rise to pollen tetrads in *qrt* strains may ultimately provide the means for performing tetrad analysis in plant species other than *Arabidopsis*. The large number of chromosomal markers (now nearly 1000) coupled with the potential for tetrad analysis serve to make *Arabidopsis* a powerful system for genetic studies, comparable with more classical microbial systems.

REFERENCES AND NOTES

1. D. D. Perkins, *Genetics* **34**, 606 (1949); *ibid.* **38**, 187 (1953); *J. Cell. Compar. Physiol.* **45** (suppl. 2), (1955); R. K. Mortimer and D. Schild, in *The Molecular Biology of the Yeast Saccharomyces. Life Cycle and Inheritance*, J. N. Strathern, E. W. Jones, J. R. Broach, Eds. (Cold Spring Harbor Laboratory, Cold Spring Harbor, NY, 1981), pp. 11–26; S. Fogel, R. K. Mortimer, K. Lusnak, *ibid.*, pp. 289–339.

2. D. D. Perkins, *Genet. Res.* **3**, 315 (1962); *Genetics* **77**, 459 (1974).
3. Mutagenized seed stocks were obtained from Lehle Seeds (Tucson, AZ), and pollen from M2 individuals was examined in a dissecting microscope. In an initial screen of 800 plants, two independent mutations, *qrt1* and *qrt2*, were identified. Subsequent screening has yielded a total of four isolates with the *quartet* phenotype from 2800 M2 strains.
4. D. Preuss, S. Y. Rhee, R. W. Davis, data not shown. Pollen viability was determined by staining with fluorescein diacetate [J. Heslop-Harrison and Y. Heslop-Harrison, *Stain Technol.* **45**, 115 (1970); S. M. Regan and B. A. Moffatt, *Plant Cell* **2**, 877 (1990)]. Mechanical separation of tetrads was performed by several passages through a pipette.
5. Polymerase chain reaction mapping markers were as described by A. Konieczny and F. M. Ausubel [*Plant J.* **4**, 403 (1993)]. The *qrt* isolates (Landsberg ecotype) were crossed to a wild-type Columbia strain, and mutant F_2 segregants were scored. For *QRT1*, linkage to *DFR* (10 recombinants/48 total) and to *LFY3* (4 recombinants/50) was observed. *QRT2* is tightly linked to *GAPC* (1 recombinant/60). The indicated map positions correspond to those listed in AATDB version 1.3 [J. M. Cherry, S. W. Cartinhour, H. M. Goodman, *Plant Mol. Biol. Rep.* **10**, 308 (1992)].
6. D. Twell, R. Wing, J. Yamaguchi, S. McCormick, *Mol. Gen. Genet.* **217**, 240 (1989); D. Twell, J. Yamaguchi, S. McCormick, *Development* **109**, 705 (1990).
7. For plant transformations, a binary Ti vector containing the LAT52-GUS transgene (6) was introduced into the *Agrobacterium* strain GV3101 that contained the helper plasmid pMP90 [C. Koncz and J. Schell, *Mol. Gen. Genet.* **204**, 383 (1986)]. Self-pollination of a GUS/+ heterozygote yielded approximately 1/4 GUS/GUS progeny, 1/2 GUS/+, and 1/4 +/+, (with a segregation ratio of 6:16:6), indicating that the transgene had integrated at a single chromosomal locus.
8. Pollen grains were incubated for 20 min in 90% (v/v) acetone, mounted and air-dried on a glass slide, and then incubated for >5 hours in 50 mM sodium phosphate buffer, 5 mM potassium ferrocyanide, 5 mM potassium ferricyanide, and X-gluc [5-bromo-4-chloro-3-indolyl glucuronide],

(0.5 mg/ml) pH 7.0 [R. A. Jefferson, *Plant Mol. Biol. Rep.* **5**, 387 (1987)]. In negative controls, pollen from plants that did not inherit the GUS transgene remained unstained (Fig. 1H).

9. S. M. Regan and B. A. Moffatt, *Plant Cell* **2**, 877 (1990).
10. S. McCormick, *ibid.* **5**, 1265 (1993); J. P. Mascarenhas, *ibid.*, p. 1303.
11. D. Preuss, B. Lemieux, G. Yen, R. W. Davis, *Genes Dev.* **7**, 974 (1993).
12. Whole pistils were fixed 3 days after pollination (11), and the callose (β -1 \rightarrow 3 glucan) within the pollen tube wall was visualized by staining with aniline blue [W. Eschrich and H. B. Currier, *Stain Technol.* **39**, 303 (1964)]. In every case, the pollen tubes observed were initiated by the grains in the tetrad, and not by contaminating pollen grains.
13. E. Knapp, *Can. J. Genet. Cytol.* **2**, 89 (1960).
14. S. Blackmore and P. R. Crane, in *Ontogeny and Systematics*, C. J. Humphries, Ed. (Columbia Univ. Press, New York, 1988), pp. 83–115.
15. Pollen grains were fixed in 2.5% glutaraldehyde as described (11), dehydrated in a graded series (30, 50, 70, 80, 95, and 100%) of ethanol, and infiltrated with L. R. White resin (Polysciences) as described by the manufacturer. The resin was polymerized by incubation at 60°C for 24 hours. Sections of 2 to 3 μ m were cut with a glass knife and mounted on glass slides. Aniline blue staining was performed as described (11).
16. H. Steiglitz, *Dev. Biol.* **57**, 87 (1977).
17. We thank A. Lloyd and R. Meagher for donating GUS transformants, D. Lashkari for providing polymerase chain reaction primers, F. Thomas for assistance with scanning electron microscopy, S. McCormick for the LAT52 promoter, and D. Botstein, D. Perkins, V. Walbot, J. McCusker, M. Raizada, and D. Ehrhardt for helpful discussions. D.P. was supported by an NSF postdoctoral fellowship and S.Y.R. was supported by an NSF predoctoral fellowship and by a Department of Energy-NSF-U.S. Department of Agriculture Training Program in Plant Biology. Supported by NSF grant MCB-91060 to R.W.D.

21 January 1994; accepted 29 March 1994

Liquid-Crystalline Mesophases of Plasmid DNA in Bacteria

Ziv Reich, Ellen J. Wachtel, Abraham Minsky*

Bacterial plasmids may often reach a copy number larger than 1000 per cell, corresponding to a total amount of DNA that may exceed the amount of DNA within the bacterial chromosome. This observation highlights the problem of cellular accommodation of large amounts of closed-circular nucleic acids, whose interwound conformation offers negligible DNA compaction. As determined by x-ray scattering experiments conducted on intact bacteria, supercoiled plasmids segregate within the cells into dense clusters characterized by a long-range order. In vitro studies performed at physiological DNA concentrations indicated that interwound DNA spontaneously forms liquid crystalline phases whose macroscopic structural properties are determined by the features of the molecular supercoiling. Because these features respond to cellular factors, DNA supercoiling may provide a sensitive regulatory link between cellular parameters and the packaging modes of interwound DNA in vivo.

The problem of DNA storage transcends the specific topic of plasmid packaging: Most extrachromosomal DNA, including

many viruses, mitochondrial and chloroplast DNA, as well as substantial portions of the prokaryotic chromosomal DNA, adopts a nucleosome-free interwound conformation (1). In contrast to the solenoidal DNA organization encountered in nucleosomal complexes, such a conformation pre-

Department of Organic Chemistry, Weizmann Institute of Science, Rehovot 76100, Israel.

*To whom correspondence should be addressed.

cludes efficient packaging (2). How does the cellular system cope, therefore, with the requirement to accommodate a large number of DNA molecules that do not present a packed nucleosomal organization?

X-ray scattering measurements made on intact bacteria carrying a high-copy plasmid revealed a relatively weak but distinct band at a reciprocal spacing of $1/51.5 \text{ \AA}^{-1}$ (Fig. 1). When the plasmid-carrying bacteria were treated early during logarithmic growth with the protein-synthesis inhibitor chloramphenicol, a substantially stronger diffraction peak centered at $1/49.1 \text{ \AA}^{-1}$ was observed. Similar spacings have been detected in cholesteric phases of DNA molecules *in vitro* and have been shown to reflect DNA-DNA interhelical interactions (3). In clear contrast, no diffraction maxima were exhibited by nontransformed cells. These results strongly suggest that the scattering profile shown in Fig. 1 reflects an ordered organization of the plasmids within the cells. The half-width of the scattering peak exhibited by the transformed, chloramphenicol-treated bacteria corresponds to a minimum effective domain size of 550 \AA (4), thus indicating a significant degree of long-range lateral order. The enhanced

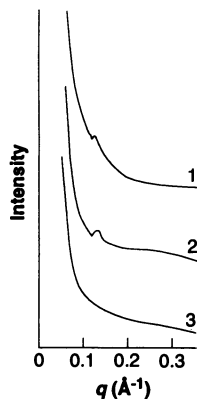
intensity of this peak relative to the peak characterizing transformed cells that have not been treated with chloramphenicol is attributed to a higher plasmid copy number, as well as to a reduced protein-related interference with the DNA ordered arrangement. The scattering maxima revealed by plasmid-carrying bacteria were found to weaken during the x-ray measurements. This decay, presumably a result of radiation-induced DNA single-strand breaks that result in the relaxation of the supercoiled topomers, suggests a supercoiling-dependent mode of plasmid organization that is progressively eliminated as an increasing number of plasmids are nicked (5).

Aqueous solutions containing isolated plasmid at physiological DNA concentrations spontaneously formed spherulites, highly birefringent domains of oily streaks, finely striated textures, and regularly spaced fringe patterns (Fig. 2). A transition into an isotropic phase occurred upon heating the sealed sample to 78°C ; the birefringent textures reappeared as the solution was cooled below the clearing point. Under identical conditions of DNA concentration and ionic strength, the open, linear form of the plasmid did not exhibit birefringent textures. DNA concentrations of 10 to 25 mg/ml correspond to the lowest estimates of DNA packaging densities within bacterial

nucleoids (6)—or of high-copy plasmids within the bacterial cytoplasmic compartment. Thus, the textures depicted in Fig. 2 indicate that supercoiled plasmids spontaneously form a liquid crystalline phase at physiological DNA concentrations. The propensity of interwound DNA conformations to promote the formation of the mesophase is quite robust: Such phases were obtained under a wide range of salt concentrations, as well as in the presence of dehydrating agents (Fig. 2). Moreover, previously characterized mesophases of linear DNA molecules have been observed only at nucleic acid densities exceeding 100 mg/ml (7, 8), whereas plasmid solutions exhibited spherulites and birefringent domains already at DNA concentrations of 10 mg/ml . Notably, higher plasmid concentrations have been shown to promote the formation of two-dimensional hexagonal assemblies (9).

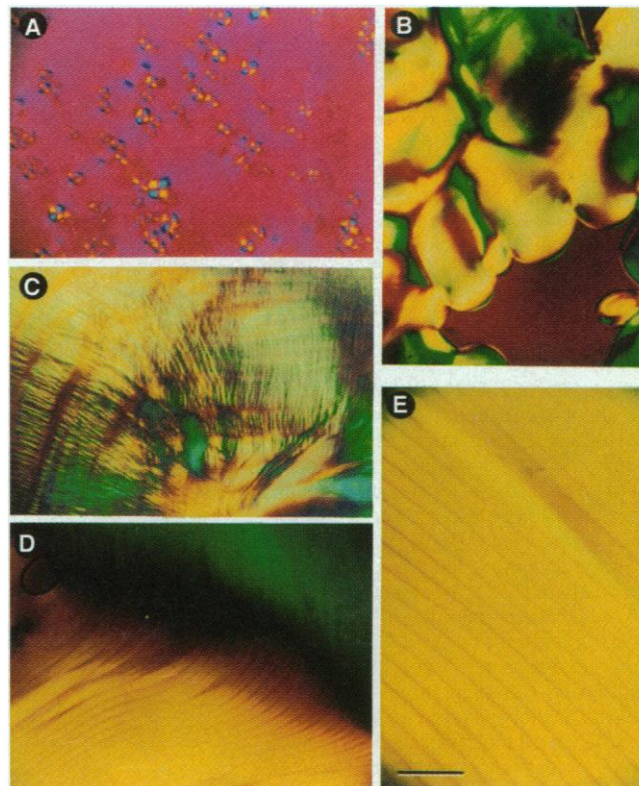
The birefringent patterns shown in Fig. 2 do not allow an unambiguous assignment of the mesophase; however, the periodic patterns [referred to as strain textures (10)], as well as the rigid, rodlike chiral nature of the plasmids, strongly suggest a cholesteric phase. Such a phase is characterized by very large nonconservative circular dichroism (CD) signals that originate from the tight molecular packaging and the long-range chiral arrangement (8, 11, 12). Indeed,

Fig. 1. X-ray scattering profiles from intact *E. coli* JM109 cells, presented in arbitrary intensity units as a function of $q = 4\pi \sin \theta/\lambda$, where q is the momentum transfer, θ is one-half the scattering angle, and λ represents the x-ray wavelength. Curve 1, *E. coli* carrying the high-copy Blue-Script plasmid (2960 base pairs); curve 2, *E. coli* carrying the Blue-Script plasmid and



treated with chloramphenicol ($150 \mu\text{g/ml}$) early during logarithmic growth; curve 3, as in curve 2 but with no *E. coli* carrying the high-copy plasmid. Specimens consisted of pellets prepared from 10-ml cultures of bacteria that were harvested early during logarithmic growth (optical density at $600 \text{ nm} = 0.3$). To minimize radiation-induced damage and to obtain a higher density of bacteria within the pellets, we treated the pellets with 2% glutaraldehyde in 0.1 M sodium cacodylate ($\text{pH } 7.4$); similar scattering profiles were obtained without glutaraldehyde but upon equilibration with 25% polyethylene glycol (28). We examined three to five independently prepared samples of each category. X-ray measurements were conducted with a low-angle camera operating with $\text{Cu-K}\alpha$ radiation, monochromated with a Ni filter followed by a single Franks mirror. Scattering profiles were recorded with a linear position-sensitive detector; data acquisition time was 16 hours.

Fig. 2. Liquid-crystalline phases of plasmid DNA observed by polarized-light microscopy at 25°C . Solutions of 10 mg/ml (A and B) or 25 mg/ml (C through E) DNA in 10 mM MgCl_2 were deposited between a slide and cover slip that were immediately and completely sealed with Torr-Seal (Varian). Gel electrophoresis of the plasmids verified that the plasmid preparations contained more than 95% closed-circular supercoiled species. Samples shown in (A) through (D) were prepared at $\text{pH } 7.0$, whereas the sample shown in (E) was at $\text{pH } 10.6$. The periodic patterns (D and E) are similar to strain textures characteristic of cholesteric phases (10). Identical patterns were obtained when samples were prepared in the presence of 0.8 M NaCl or of 20% ethanol. Specimens were observed through crossed polarizers with the use of a quartz retardation plate at an angle of 45° relative to the samples and a Zeiss microscope (Zeiss, Oberkochen, Germany) equipped with a Mettler FP5 thermostat (Mettler-Toledo, Greifensee, Switzerland). Bar, $20 \mu\text{m}$.



appropriate conditions of salt and dehydrating agents have been found to effect packaging of linear DNA molecules into chiral, tightly packed aggregates. The anomalous ellipticities exhibited by these aggregates were attributed to the formation of cholesteric microdomains whose molecular organization—and hence the resulting spectroscopic properties—is identical to that of the cholesteric macrodomains (11). Dilute solutions of supercoiled plasmids also exhibited, under packaging conditions, large nonconservative CD signals (Fig. 3, curves 1 to 3). This observation indicates that, in addition to a macroscopic liquid crystalline organization, closed-circular supercoiled DNA molecules can form cholesteric microdomains, provided that a critical local DNA concentration has been effected by condensing agents.

The sign of the nonconservative ellipticities exhibited by a cholesteric organization reflects the sense of the cholesteric twist: positive nonconservative CD signals correspond to a right-handed long-range chirality, whereas negative signals are associated with a left-handed twist (12). The sense of the cholesteric twist in lyotropic phases of

helical polymers depends, in turn, on the handedness of the molecule—right-handed helices stabilize a left-handed cholesteric configuration [Rudall's rule (8, 13)]—and, predominantly, on the dielectric properties of the medium (14, 15). Indeed, the long-range twist in cholesteric phases of a given polypeptide (14) or in packed chiral forms of linear DNA segments [such as the open derivatives of the plasmid (Fig. 3, curves 1' to 3')] depends solely on the packaging medium, which modifies the dipole interactions within the molecules but does not alter their helical sense.

Native, closed-circular DNA molecules exhibit a negative, right-handed supercoiling. Because the linking number (16) is a topological invariant, conditions that promote DNA unwinding, such as a temperature- and pH-induced partial melting of the double strands (17) or binding of intercalating drugs (18), progressively decrease the twist within the double-stranded DNA and hence gradually reduce the negative supercoiling density. Notably, the reduced superhelical density is associated with a pronounced increase of the plasmid diameter (2, 19). We find that modifications of the

supercoiling parameters affect the properties of the ordered plasmid aggregates.

A left-handed long-range cholesteric twist, induced and stabilized by the plasmid native right-handed superhelicity (8, 13), was indicated by the large negative nonconservative ellipticities exhibited by the plasmid aggregates (Fig. 3). An increased cholesteric pitch results in a substantially increased magnitude of the CD signals displayed by cholesteric phases (20). Indeed, those factors that act to enlarge the pitch of the plasmid-derived cholesteric aggregates by reducing the plasmid superhelical density (that is, increased temperature and pH values or intercalation) and hence increasing its diameter, were found to cause an increase in the magnitude of the CD signals (21) (Fig. 4, A, B, and D). The nonchiral nematic configuration associated with a complete relaxation of the supercoiling was indicated by the elimination of the nonconservative ellipticities. The large, positive, nonconservative CD signals observed upon a further increase of the temperature or of the pH values (Fig. 4, A and B) point toward a right-handed cholesteric organization that is associated with a positive, left-handed, superhelical sense (13). Although a pH-induced right-to-left reversal of the supercoiling handedness has not been documented and was not substantiated with direct experimental evidence here, we suggest that the results depicted in Fig. 4 might be ascribed to the induction of a low-density positive superhelicity (22).

This speculation is supported by the observation that the supercoiling-dependent alterations of the plasmid supramolecular organization are reversible: the right-handed cholesteric twist, which stems from the left-handed superhelicity proposed to characterize plasmids at relatively high pH values, was eliminated and finally reversed upon progressive cooling of the sample, as indicated by the reversal of the nonconservative ellipticities (Fig. 4C). Indeed, by promoting DNA annealing and thus reversing the pH-induced melting, the cooling acts to increase the twist and to induce a left-to-right change of the supercoiling sense. A strict correlation can be observed between the macroscopic properties of the organization adopted by interwound DNA on one hand, and the density and handedness of the molecular superhelicity on the other.

Plasmid DNA molecules are shown here to segregate into ordered, supercoiling-mediated clusters within bacteria; *in vitro* observations suggest that such clusters assume a cholesteric organization. Whereas the parameters of all previously characterized lyotropic cholesteric phases of biomacromolecules revealed a rather unpredictable dependence on the molecular properties of their

Fig. 3. CD spectra exhibited by aggregates of plasmid DNA ($\Delta\epsilon$, molar ellipticity). DNA concentrations in all samples was 35 $\mu\text{g/ml}$ (5×10^{-5} M, in base pairs). Curve 1, 0.8 M NaCl and 35% ethanol; curve 2 2.2 M NaCl and 35% ethanol; curve 3, 10 mM MgCl_2 and 20% ethanol; curve 4, 10 mM MgCl_2 . The solid curves (1 to 3) are CD spectra of the closed-circular plasmids; broken lines (curves 1' to 3') represent spectra of the open, linearized plasmid forms, whereas the conservative curve 4 characterizes both the closed and open forms. Spectra were recorded at room temperature on a Jasco J-500 spectropolarimeter equipped with a DP-500 data processor (Japan Spectroscopic Co., Tokyo) and a NESLAB circulating bath for temperature control.

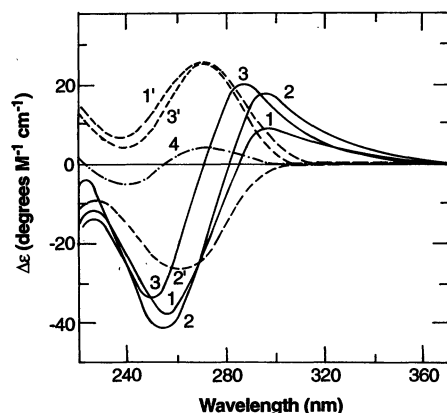
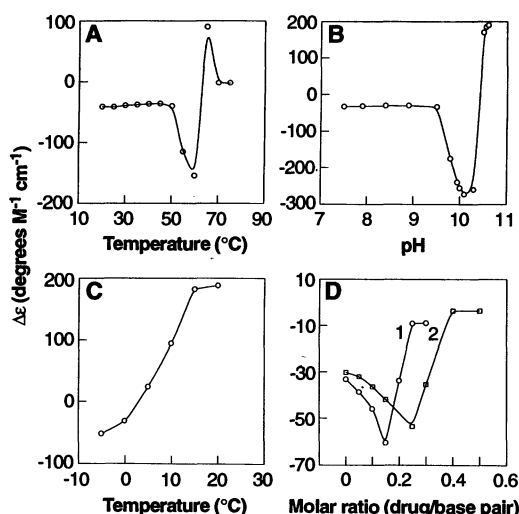


Fig. 4. Effects of DNA-unwinding factors on the optical properties of the liquid crystalline phases derived from the closed-circular plasmids. Graphs represent CD maxima exhibited by the plasmid chiral organizations under the following conditions: (A) 2.2 M NaCl and 35% ethanol, as a function of temperature; (B) 10 mM MgCl_2 and 20% ethanol, as a function of pH; (C) 10 mM MgCl_2 and 20% ethanol at pH 10.6, as a function of temperature; and (D) 10 mM MgCl_2 and 20% ethanol, with (1) actinomycin or (2) ethidium bromide (29), as a function of the molar ratio of drug to base pairs. Unless otherwise stated, samples were measured at room temperature and at pH 7.0. Each data point on the curves shown in (B) and (D) represents a CD maximum obtained from an independently prepared sample.



constituent species, the macroscopic features of the liquid-crystalline phases obtained from interwound DNA were found to be directly and exclusively determined by the density and handedness of the supercoiling. Because the supercoiling density responds to environmental and genetic parameters (23), we propose that in addition to its role in genetic transactions (24), DNA supercoiling promotes ordered DNA segregation and serves as a regulatory link between cellular determinants and DNA supramolecular packaging. The demonstrated propensity of supercoiled DNA species to form liquid crystalline phases and to regulate their properties—in vitro as well as in bacteria, viruses (25), and mitochondria (26)—is consistent with the notion that supercoiling-dependent liquid crystallinity provides an effective and general packaging mode for interwound, nucleosome-free DNA molecules in vivo.

REFERENCES AND NOTES

- W. R. Bauer, F. H. C. Crick, J. H. White, *Sci. Am.* **243**, 100 (July 1980); G. Yagil, *Crit. Rev. Biochem. Mol. Biol.* **26**, 475 (1991).
- T. C. Boles, J. H. White, N. R. Cozzarelli, *J. Mol. Biol.* **213**, 931 (1990).
- D. Durand, J. Doucet, F. Livolant, *J. Phys. France* **2**, 1769 (1992); T. P. Maniatis, thesis, Vanderbilt University, Nashville, TN (1971).
- We calculated this with the Sherrer equation [N. M. Henry, H. Lipson, W. A. Wooster, *The Interpretation of X-ray Diffraction Photographs* (Macmillan, London, 1961), pp. 212–218].
- In vitro CD studies conducted on nicked-circular DNA molecules (obtained by exposing the supercoiled plasmids to a moderate deoxyribonuclease I activity) indicated that these species do not aggregate into chiral clusters (27). This result supports the assumption that radiation-induced DNA nicking is responsible for the time-dependent decay of the scattering peak.
- E. Kellenberger *et al.*, in *Bacterial Chromatin*, G. O. Gualerzi and C. I. Pon, Eds. (Springer-Verlag, Berlin, 1986), pp. 11–27; E. Kellenberger, *Trends Biochem. Sci.* **12**, 105 (1987); E. Kellenberger and B. A.-S. Gahmen, *Microbio. Lett.* **100**, 361 (1992).
- F. Livolant, *Eur. J. Cell Biol.* **33**, 300 (1984); R. L. Rill, *Proc. Natl. Acad. Sci. U.S.A.* **83**, 342 (1986); T. E. Strzelecka and R. L. Rill, *J. Am. Chem. Soc.* **109**, 4513 (1987); F. Livolant, *J. Physique* **48**, 1051 (1987); T. E. Strzelecka, M. W. Davidson, R. L. Rill, *Nature* **331**, 457 (1988); Y. M. Yevdokimov, S. G. Skuridin, V. I. Salyanov, *Liq. Cryst.* **3**, 1443 (1988); F. Livolant, A. M. Levelut, J. Doucet, J. P. Benoit, *Nature* **339**, 724 (1989); D. H. Van Winkle, M. W. Davidson, W. X. Chen, R. L. Rill, *Macromolecules* **23**, 4140 (1990); F. Livolant, *J. Mol. Biol.* **218**, 165 (1991); A. Leforestier and F. Livolant, *Biol. Cell.* **71**, 115 (1991).
- F. Livolant and M. F. Maestre, *Biochemistry* **27**, 3056 (1988).
- J. Torbet and E. DiCapua, *EMBO J.* **8**, 4351 (1989).
- G. S. Chilaya and L. N. Lisetski, *Mol. Cryst. Liq. Cryst.* **140**, 243 (1986).
- D. Keller and C. Bustamante, *J. Chem. Phys.* **84**, 2972 (1986); C. Bustamante, B. Samori, E. Builes, *Biochemistry* **30**, 5661 (1991).
- C. Reich, M. F. Maestre, S. Edmondson, D. M. Gray, *Biochemistry* **19**, 5208 (1980); M. F. Maestre and C. Reich, *ibid.*, p. 5214.
- K. M. Rudall, *Lect. Sci. Basis Med.* **5**, 217 (1955).
- C. Robinson, *Tetrahedron* **13**, 219 (1961).
- T. V. Samulski and E. T. Samulski, *J. Chem. Phys.* **67**, 824 (1977); E. T. Samulski and A. V. Tobolsky, in *Liquid Crystals and Plastic Crystals*, G. W. Gray and P. A. Winsor, Eds. (Horwood, Chichester, 1974), vol. 1, p. 175.
- The degree and sense of supercoiling in interwound DNA species are defined by the relation $Lk = Tw + Wr$ (16), where Lk is the linking number, Tw is the twist of the DNA strands, and Wr , or writhe, provides the extent and handedness of the supercoiling [J. H. White, *Am. J. Math.* **91**, 693 (1969)].
- J. Vinograd, J. Lebowitz, R. Watson, *J. Mol. Biol.* **33**, 173 (1968); J. C. Wang, *ibid.* **43**, 25 (1969); F. S. Lee and W. R. Bauer, *Nucleic Acids Res.* **13**, 1665 (1985); R. Bowater, F. Abdul-ela, D. M. J. Lilley, *Biochemistry* **30**, 11495 (1991).
- M. Waring, *J. Mol. Biol.* **54**, 247 (1970).
- A. V. Vologodskii, S. L. Levene, K. V. Klenin, M. F. Kamenetskii, N. R. Cozzarelli, *ibid.* **227**, 1224 (1992).
- M.-H. Kim, L. Ulbarri, D. Keller, M. F. Maestre, C. Bustamante, *J. Chem. Phys.* **84**, 2981 (1986).
- Our proposed correlation between a decreased superhelical density and increased magnitudes of the cholesteric optical properties is supported by the enhanced CD signals exhibited under packaging conditions by partially relaxed topoisomers, obtained by use of topoisomerase II; the magnitude of these signals is four to five times larger than that of those displayed by native, nonrelaxed plasmids (27).
- The previously reported dependence of twist handedness in cholesteric liquid crystals on the helical sense of polymers that form this phase (13) corroborates the assumption that a right-to-left reversal of the supercoiling sense does indeed occur at moderately elevated pH values. Notably, for a supercoiling density of 0.05 (characteristic of isolated plasmids), only 150 base pairs, which constitute 5% of the plasmid total length, must be titrated to effect complete relaxation; additional titration of a few base pairs would lead to a low positive superhelical density. Such a limited titration can be done at a moderately elevated pH [J. C. Wang, *J. Mol. Biol.* **89**, 783 (1974)]. The very large positive CD signals observed under packaging conditions at these pH values are clearly inconsistent with the occurrence of extensive DNA denaturation and point toward a right-handed cholesteric twist.
- J. M. McClellan, P. Boubliková, E. Palecek, D. M. J. Lilley, *Proc. Natl. Acad. Sci. U.S.A.* **87**, 8373 (1990); K. Drlica, *Mol. Microbiol.* **6**, 425 (1992).
- R. Kannar and N. R. Cozzarelli, *Curr. Opin. Struct. Biol.* **2**, 369 (1992); J. C. Wang and A. S. Lynch, *Curr. Opin. Gene Dev.* **3**, 764 (1993).
- J. Lepault, J. Dubochet, W. Baschong, E. Kellenberger, *EMBO J.* **6**, 1507 (1987); F. P. Booy *et al.*, *Cell* **64**, 1007 (1991).
- G. Brugerolle and J. P. Mignot, *Biol. Cell.* **35**, 111 (1979).
- Z. Reich and A. Minsky, unpublished results.
- The osmotic pressure exerted by 25% (w/w) polyethylene glycol is comparable to the osmotic pressure within *Escherichia coli* cells [P. Mitchell and J. Moyle, in *Bacterial Anatomy*, 6th symposium of the Society for General Microbiology, E. T. C. Spooner and B. A. D. Stocker, Eds. (Cambridge Univ. Press, Cambridge, 1956), vol. 6, pp. 150–179]. Thus, polyethylene glycol should not effect ordered DNA packaging within bacteria.
- We derived binding constants of ethidium bromide to supercoiled DNA molecules under the specific experimental conditions used for the reported CD studies by determining the concentration of unbound ethidium bromide. Under such conditions, the drug to base pair molar ratio of 0.4 (at which the plasmid-derived liquid-crystalline phase is no longer chiral) corresponds to a binding ratio of 0.05, which was found to induce plasmid relaxation (18), thus supporting the suggested correlation between the supercoiling parameters and the properties of the plasmid cholesteric organization.
- We thank S. L. Zaidman and M. Zohar for technical assistance. A.M. is an incumbent of the Victor L. Ehrlich Career Development Chair. Supported by a grant from the Minerva Foundation, Germany.

5 January 1994; accepted 28 April 1994

Activation of Raf as a Result of Recruitment to the Plasma Membrane

David Stokoe, Susan G. Macdonald, Karen Cadwallader, Marc Symons, John F. Hancock*

The small guanine nucleotide binding protein Ras participates in a growth promoting signal transduction pathway. The mechanism by which interaction of Ras with the protein kinase Raf leads to activation of Raf was studied. Raf was targeted to the plasma membrane by addition of the COOH-terminal localization signals of K-ras. This modified form of Raf (RafCAAX) was activated to the same extent as Raf coexpressed with oncogenic mutant Ras. Plasma membrane localization rather than farnesylation or the presence of the additional COOH-terminal sequence accounted for the activation of RafCAAX. The activation of RafCAAX was completely independent of Ras; it was neither potentiated by oncogenic mutant Ras nor abrogated by dominant negative Ras. Raf, once recruited to the plasma membrane, was not anchored there by Ras; most activated Raf in cells was associated with plasma membrane cytoskeletal elements, not the lipid bilayer. Thus, Ras functions in the activation of Raf by recruiting Raf to the plasma membrane where a separate, Ras-independent, activation of Raf occurs.

Ras functions in a signal transduction pathway from the cell membrane to the nucleus. Binding of growth factors to their

receptors results in receptor dimerization and autophosphorylation of tyrosine residues in the cytoplasmic tail of the receptor. Among the multiple proteins that bind to the phosphorylated tail of the epidermal growth factor receptor is the Grb2-Sos complex. The translocation of Sos to the plas-

ONXY Pharmaceuticals, 3031 Research Drive, Richmond, CA 94806, USA.

*To whom correspondence should be addressed.